Prediction of formation of cubic boron nitride by construction of temperature–pressure phase diagram at the nanoscale

Shengliang Hu [a,b,*], Jinlong Yang [b], Wei Liu [b], Yingge Dong [b], Shirui Cao [b], Jun Liu [a]

[a] *Science and Technology on Electronic Test and Measurement Laboratory, Key Laboratory of Instrumentation Science & Dynamic Measurement (North University of China), Ministry of Education, Taiyuan 030051, PR China*
[b] *School of Materials Science and Engineering, North University of China, Taiyuan 030051, PR China*

ARTICLE INFO

ABSTRACT

The size-dependent phase diagram of BN was developed on the basis of the nanothermodynamic theory. Our studied results suggest that cubic BN (c-BN) is more stable than hexagonal BN (h-BN) in the deep nanometer scale and the triple point of c-BN, h-BN and liquid shifts toward the lower temperature and pressure with decreasing the crystal size. Moreover, surface stress, which is determined by the experimental conditions, is the main reason to influence the formation of c-BN nuclei. The developed phase diagram of BN could help us to exploit new techniques for the fabrication of c-BN nanomaterials.

1. Introduction

Boron nitride (BN) is similar to carbon with two crystalline structures: a layered hexagonal structure (h-BN), which is similar to that of graphite, and the cubic zinc-blende structure (c-BN), analogous to that of diamond [1]. Therefore, c-BN shares many similar attractive properties of diamond and shows high potential for mechanical, electrical and optical applications [1,2]. Although c-BN was prepared by the high-pressure and high-temperature method in 1957 [3], many attentions of developing facile and economical c-BN preparations have been paid for 50 years. It is well known that phase diagram is helpful in predicting phase transformations and the resulting microstructures. Accordingly, the pressure–temperature (P–T) phase diagram of BN was attempted to be constructed immediately by Wentorf after his synthesis of c-BN, and then was improved by Corrigan and Bundy in 1963 [4,5]. Subsequently many researchers attempt to refine the BN phase diagram on the basis of experimental data and thermodynamic approach [6–10].

Fig. 1 is the last BN equilibrium phase diagram from Solozhenko et al. [8]. However, this phase diagram cannot explain the phenomena that the formation regions of c-BN nuclei produced from many synthesized methods, such as ion-assisted chemical vapor deposition

(CVD), ion-assisted physical vapor deposition (PVD) [2] and super-critical-fluid system [11,12], are located below the phase equilibrium line of the present BN phase diagram, where h-BN is a thermo-dynamically stable rather than the c-BN. Why would the present phase diagram of BN be not suitable for the synthesized methods mentioned above? It is well known that the size of critical nuclei is limited in several nanometer scales upon vapor-phase nucleation systems (such as ion-assisted CVD and PVD), the amount of grain boundaries in c-BN nanofilms is rather high, and therefore these materials should be called nanometer c-BN [2,13]. For the super-critical fluid synthesis, Horiuchi et al. had pointed out that the size of c-BN nuclei was in the range of 2–8 nm [11,12]. Consequently, the size effect on the formation of c-BN in the deep nanometer scale may be involved.

It is now known that the thermal properties, for example, the melting temperature, of all low-dimensional crystals depend on their size [14]. For free standing nanocrystals, the melting temperature decreases as its size reduces. For nanocrystals embedded in a matrix, they could melt below or above the melting point of the corresponding bulk crystal that is determined by the interface structure between embedded nanocrystals and the matrix [14,15]. If the interface is coherent or semi-coherent, there is an increase in the melting point. Otherwise, a depression of the melting point is present [16]. Some molecular dynamics simulations indicated that the free clusters exhibit a depression of the melting point with decreasing the size while embedded or coated clusters show superheating [15,17]. A thermodynamic calculation of size-dependent melting point was carried out by
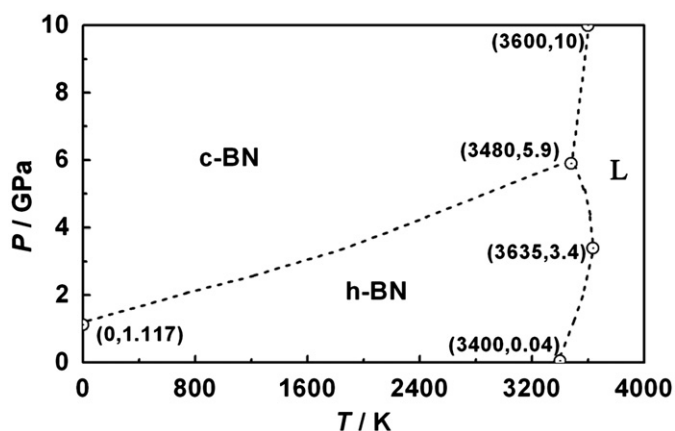
Fig. 1. Last temperature–pressure phase diagram of bulk BN proposed by Solozhenko et al.

Pawlow and Hanszen, and then developed recently by Jiang et al. [14,18–20]. The developed thermodynamic model can predict the size-dependent melting point for various low-dimensional crystals. Furthermore, the thermodynamic theory can also explain the phase stability of solid nanocrystals by taking into account the size-dependence of the surface stress of nanocrystals [21]. Accordingly, herein we propose a thermodynamic method to establish the size-dependent phase diagram of BN. In particular, this developed phase diagram of BN can be used to predict the nanosized c-BN formation under the low-pressure synthesis methods, which might help us to exploit new techniques for the fabrication of c-BN nanomaterials.

2. Theory description

As for a nanostructure, it can be understood not only as the structure of a single nanoparticle, but also as a structure formed by a conglomerate of nanoparticles of any sizes [22]. A distinctive characteristic of a nanoparticle is the dependence of its properties on the particle size, which is recognized still in the classical theory of capillary by the Laplace–Young equation: $\Delta P = 4f/d$, where f denotes the surface stress and d is the particle diameter [22,23]. For the internal mechanical state of a nanoparticle, the surface stress of the first monolayer is important. Therefore, the surface stress could influence on phase transition in nanoparticles. However, due to its small size, a nanoparticle changes its phase state practically instantaneously so that it is hard to image the state of equilibrium between two phases inside the particle [22]. In this case, it is more reasonable to construct size-dependent BN phase diagram on the basis of its bulk phase transition boundaries.

Since the bulk BN phase diagram has been provided by the previous researchers [4–10] (as shown in Fig. 1), the details of the bulk phase transition boundaries between h-BN and c-BN phase (denotation by hc), h-BN and liquid phase (denotation by hL), and c-BN and liquid phase (denotation by cL), respectively, can be obtained and showed in the following:

$$T_{hc}(\infty,P) = -812.703 + 727.577P \tag{1}$$

$$T_{hL}(\infty,P) = \begin{cases} 3397.202 + 69.94P \to 0.04 \leq P \leq 3.4 \\ 3845.8 - 62P \to 3.4 < P \leq 5.9 \end{cases} \tag{2}$$

$$T_{cL}(\infty,P) = 3307.32 + 29.268P \tag{3}$$

In order to distinguish from the nanosystem, the symbol of ∞ in the above equations denotes the bulk phase materials.

If a nanoparticle is subjected to external mechanical actions considered to be uniform along the nanoparticle surface for the sake of simplicity; the stable state of the nanoparticle must be not only related to the surrounding conditions, but also dependent on the surface stress [22]. For a spherical and isotropic BN nanocrystal with a diameter d, it must be subjected to the surrounding pressure P and an excess pressure ΔP created by surface stress in a solid particle. The total pressure P_t can be expressed as $P_t = \Delta P + P$. Accordingly, there are two extreme cases: one is $\Delta P \approx 0$, i.e. $P_t \approx P$ with $d \to \infty$, this case suggests the normal situation of pressure-dependent solid–solid phase transition for bulk materials; the other is $P \approx 0$, $P_t \approx \Delta P$, this case is the size-dependent solid–solid phase transition for nanosized materials [24]. Hereby, the equation of $P_t = \Delta P + P$ can be applicable for bulk and nanosized materials. Based on the bulk hc phase boundary shown in Eq. (1), the size-dependent transition temperature function T_{hc} can be expressed as

$$T_{hc}(d,P) = -812.703 + 727.577(P + 4f/d) \tag{4}$$

Here, f can be determined by $f = h[(S_{vib}H_m)/(2\kappa V_m R)]^{0.5}$ [25,26], where H_m is the bulk melting enthalpy of crystals, $S_{vib}(\infty)$ is the vibrational part of the total melt entropy $S_m(\infty)$, and $S_{vib}(\infty) \approx 0.19S_m$ [26], κ is the compressibility, h is the atomic diameter and R is the ideal gas constant.

For bulk crystals, atoms in the surface layers can oscillate with large amplitude than atoms in the interior of the crystals, and the average amplitude of the whole crystal is independent on the size of the crystal [27]. However, it can be considered that in nanocrystals the atomic oscillation of large amplitude exists not only in the surface, but also in the core [27]. Thus, the melting behavior for the nanometer-size particles is expected to be size-dependent. To determine the melting temperature of h-BN, we use the Lindemann criterion, which says that a crystal will melt when the root mean-square displacement of the atoms in the crystal exceeds a certain fraction of the interatomic distance [24,27,28]. The Lindemann hypothesis is known to be valid qualitatively for nanoparticles [28,29]. Using both Lindemann criterion and Mott's equation for an isolated nanoparticle, the size-dependent melt temperature functions $T_m(d,P)$ of h-BN can be obtained as

$$T_m(d,P) = T_m(\infty,P)\exp\{-[2S_{vib}(\infty)/(3R)]/[d/(6h)-1]\} \tag{5}$$

Thus, the corresponding $T_{hL}(d,P)$ function is given as

$T_{hL}(d,P)$
$$= \begin{cases} (3397.202 + 69.94P)\exp\{-[2S_{vib}(\infty)/(3R)]/[d/(6h)-1]\} \to 0.04 \leq P(\text{GPa}) \leq 3.4 \\ (3845.8 - 62P)\exp\{-[2S_{vib}(\infty)/(3R)]/[d/(6h)-1]\} \to 3.4 < P(\text{GPa}) \leq 5.9 \end{cases}$$
$$\tag{6}$$

The triple point of h-BN, c-BN and liquid phase can be obtained when $T_{hL}(d,P)$ is equal to $T_{hc}(d,P)$ [24]. Therefore, the slope of the phase boundary between nanosized c-BN and liquid phase is expressed as

$$dT_{cL}(d,P)/dP = 29.268\exp\{-[2S_{vib}(\infty)/(3R)]/[d/(6h)-1]\} \tag{7}$$

As a result, the $T_{cL}(d,P)$ function is given as

$$T_{cL}(d,P) = T_t + 29.268\exp\{-[2S_{vib}(\infty)/(3R)]/[d/(6h)-1]\}(P-P_t) \tag{8}$$

3. Results and discussion

To plot the size-dependent phase diagram of BN, the parameters in Eqs. (4), (6) and (8) must be determined firstly. The value of h can be obtained on the basis of $h = \sqrt{3}a/4$ [25,26], where a is the lattice parameter. For c-BN, $a = 0.362$ nm, $S_m = 33.24$ J/(mol K); for h-BN, $a = 0.358$ nm, $S_m = 25$ J/(mol K) [7–10]. Since f of both c-BN and h-BN is the same on the equilibrium phase boundary, it can be
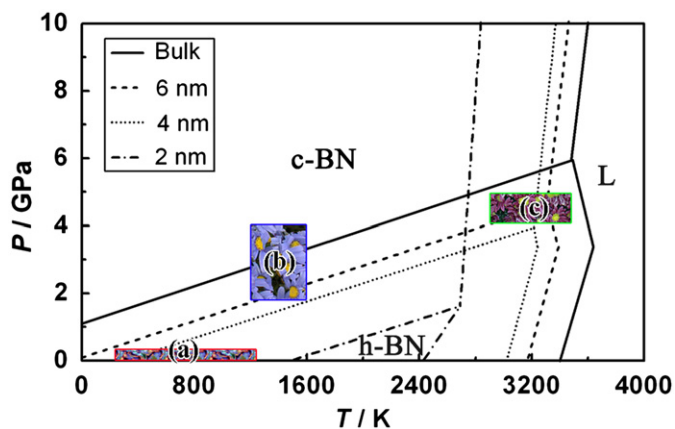
Fig. 2. Temperature–pressure phase diagrams of bulk and nanosized BN on the basis of the above model, and the condition regions of c-BN formation from low pressure CVD and PVD routes [2], supercritical-fluid systems [11] and pulsed-laser ablation in liquid [24] are marked with the colorful rectangles of (a), (b) and (c), respectively.

determined as $f = 1.6$ J/m^2 [11,21]. Therefore, the size-dependent temperature–pressure phase diagram of BN obtained from Eqs. (4), (6) and (8) is plotted in Fig. 2.

As shown in Fig. 2, it can be seen that the melting temperature of isolated BN nanoparticles decreases with decrease in d, resulting in the displacement of the triple point toward lower temperature with decrease in d. The nanosize-induced excess pressure ΔP that increases with the decrease in the crystal particle's size drives the metastable region of c-BN nucleation into the new stable region in the size-dependent P–T phase diagram of BN [30]. Therefore, when the "bottom up" methods are used to prepare nanomaterials and the size of critical nuclei can be limited in very small nanometer scales, the lower (or normal) pressure will be required for the c-BN formation. For example, various assisted CVD or PVD methods [2,31].

Presently, the previous proposed models to explain the formation of c-BN films can be classified into five groups: (a) selective sputter model; (b) thermal spike model; (c) static stress model; (d) dynamic stress model; (e) subplantation model [2,31,32]. However, it must be recognized that none of these models accounts for all the accumulated experimental results self-consistently [2]. One reason is each model focuses on a limited aspect of a complicated process involving ion damage, densification and phase transformation; the other is that the nucleation and growth stages have been dealt with within the same framework, and have not been discussed separately [2,32]. The grain sizes observed in c-BN film are quite small, ranging in diameter from a few nanometers to at most about 100 nm [32]. Grains frequently grow in a columnar morphology starting from the point of nucleation at the top of the graphitic layer and elongating towards the surface of the film [2]. This suggests that once nucleated, the c-BN grows as a single phase. Since the size of c-BN nucleation is very small and in the nanometer scale, the original development of the P–T bulk phase diagram of BN is not suited for the explanation of c-BN formation in the nucleation process. To better understand the original mechanism of c-BN formation under the low or normal pressure, it is required to develop the size-dependent phase diagram of BN. Although earlier experiments and calculations also suggest that the P–T phase boundary line between h-BN and c-BN phases should be shifted to lower pressure [33–35], which would make c-BN the thermodynamically stable phase under ambient conditions, the available phase diagram of BN can still not be established to understand the c-BN nucleation under the different conditions.

According to our constructed size-dependent phase diagram shown in Fig. 2, it can be seen that c-BN phase can be formed in various temperatures and pressures if only the size of the critical

nuclei is small enough. The previous experimental results also suggest that c-BN can be formed and grown over a wide range of temperatures and pressures. For example, the temperatures can range from room temperature to over 1000 °C and the pressures can vary from tens of Pa to several tens of GPa. In fact, there are a variety of synthesis methods that can produce the different conditions of c-BN formation, such as electron-beam evaporation plating, sputtering, radio frequency thermal plasmas, supercritical-fluid systems and pulsed-laser ablation [2,30–32]. Under supercritical-fluid conditions, for example, generally the pressure is in the range of 1.8–3.8 GPa and temperature is in the range of 1200–1600 K [11]. It can be seen that these condition regions are located below the phase transition line between h-BN and c-BN of bulk BN phase diagram reported by Corrigan and Bundy, but they are in agreement with our developed size-dependent phase diagram according to the size of c-BN (2–8 nm) generated in supercritical conditions [11]. For comparison, Fig. 2 shows the condition regions from CVD and PVD methods [2], supercritical-fluid systems [11] and pulsed-laser ablation [30], corresponding to the positions of (a), (b) and (c), respectively. Under such conditions, the formation of c-BN nuclei can be completely explained on the basis of the size-dependent P–T phase diagram of BN. However, why must the experimental conditions (e.g. ion energy and mass, substrate material, gas environments, catalysts, etc.) be controlled to fabricate c-BN in experiments and how do they influence the nucleation process of c-BN? To answer these questions, may be the surface stress f should be reconsidered as a variable.

According to the Laplace–Young equation, the value of ΔP depends on f and their corresponding relationship is shown in Fig. 3a. It can be seen that ΔP increases with the f increase and the size reduction. Since Eq. (4) can be rewritten as
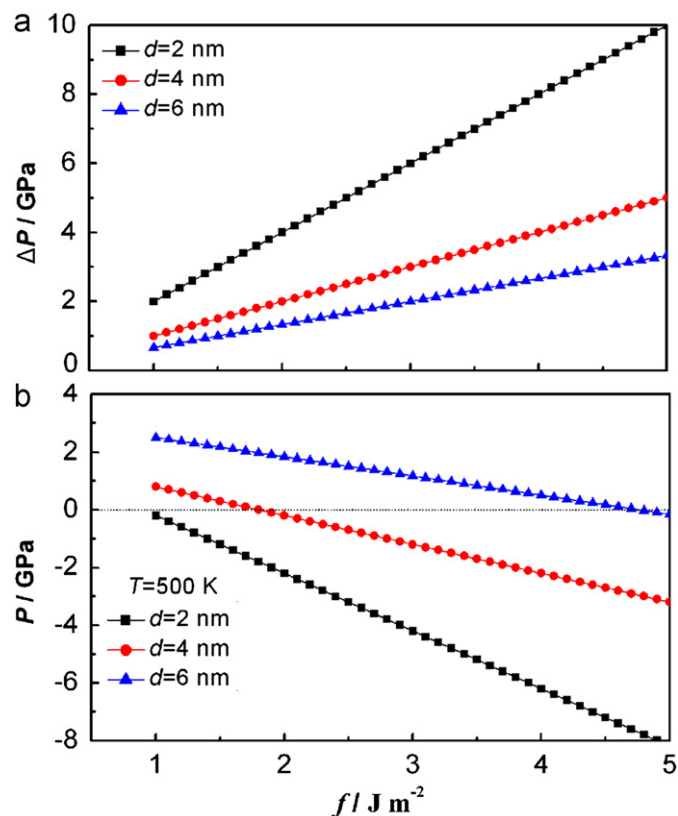

Fig. 3. (a) Relationship curves between the excess pressure (ΔP) and surface stress (f) at the given sizes; (b) dependence of the size-dependent critical pressure of solid–solid transition between h-BN and c-BN with some given sizes on the f at $T = 500$ K.

$P_{hc}(d,T) = [(T+812.703)/727.577] - 4f/d$, the dependence of the size-dependent critical pressure of solid–solid transition between h-BN and c-BN with some given sizes on the f at $T = 500$ K can be obtained as shown in Fig. 3b. One can see that the P–T phase transition boundary between h-BN and c-BN decreases with the increase in the value of f. On the other hand, according to the nucleation nanothermodynamics proposed by Yang et al. [11,21], the Gibbs free energy $\Delta G(d,P,T)$ of spherical c-BN clusters is expressed as a function of diameter d, pressure P and temperature T, as follows:

$$\Delta G(d,P,T) = \{-(\pi d^3 \Delta V[P - P_{hc}(d,T)]/6V_m + \pi d^2 \gamma\}f(\theta) \tag{9}$$

where ΔV is the molar volume difference between h-BN and c-BN, γ is the surface energy and θ is a contact angle. Based on Eq. (9), it can be seen that $\Delta G(d,P,T)$ depends on $P_{hc}(d,T)$, and its value decreases with decrease in the value of $P_{hc}(d,T)$ at the given d. In other words, the reduction of $P_{hc}(d,T)$ is in favor of the formation of c-BN nuclei. Since $P_{hc}(d,T)$ is determined by f, it can be concluded that c-BN nuclei can be formed under no outside pressures when f reaches the certain value, i.e. the c-BN formation is determined by the value of f.

Furthermore, one can see from Eq. (9) that $\Delta G(d,P,T)$ is influenced by γ. However, both f and γ are determined by the atomic energy state in the surface layer, i.e. interatomic interaction and coordination number (CN) [36]. From a fundamental point of view, nanostructures bridge the gap between an isolated atom and its bulk counterpart in its chemical and physical behavior. The key difference between a solid and its elementally isolated atom is the involvement of interatomic interaction. Compared with its bulk counterpart, a nanocrystal has a high portion of under-coordinated atoms in the surface skin. Therefore, interatomic interaction and the changing fraction of the under-coordinated atoms should be the key factors dictating why the behavior of a nanocrystal is different from that of an isolated atom or bulk counterpart [36–38]. Based on the definitions of f and γ, f gives the work required to stretch a given segment of surface, altering atomic structure, whereas γ is a positive scalar quantity that is a measure of the energy required to create a new segment of interface with the same atomic configuration [37]. In the case of liquid, f and γ are identical, but in the case of solids they are generally different. This is because the termination of the lattice periodicity in the surface normal direction, or a grain boundary, has two effects. One is the creation of the surface potential barrier (or contact surface) and the other is the reduction of the atomic CN [36,38]. The CN of an atom in a highly curves surface is lower compared with the CN of an atom at a flat surface [38]. Thus CN imperfection will shorten the remaining bonds of the under-coordinated atom, resulting in the change of atomic bonding state and influencing the physical–chemical properties of a solid material [36–38]. Recently, many efforts have been made to uncover the roles of the surface state in the thermal, mechanical and other properties [38–45]. For instance, the size effects of the nanostructures with negative curvature (such as nanocavities, nanotubes, hollow nanospheres and core–shell configuration) on the elastic modulus, the melting temperature, the surface free energy and the cohesive energy have been extensively investigated by thermodynamic theory or other theory [38–45]. According to the above analysis, it is easily understood that the value of f is variable and depends on the atomic bonding state in the surface skin.

Besides the effect of atomic CN imperfection on the value of f, the contact substances (including of gas, liquid and solid matter) on the surface of c-BN nuclei, the surrounding pressures and temperatures also contribute to this behavior [21–23]. The value of f frequently increases with increase in the interaction forces between the contact substances and the formed nuclei while decreases with the increase in the surrounding temperature and pressure. Based on such considerations, there will be different values between the gas condensation nucleation from CVD and PVD and the nucleation on crystal-melt interface from super-critical-fluid systems [2,11]. Moreover, many species like O, N, H, F, Cl and OH, which are usually bonded with c-BN, may also influence the value of f [2,31–33]. Accordingly, the facile and economical fabrication of nanosized c-BN materials would be realized by tailoring the value of f. To realize this intention, certainly, the techniques of measured f in various conditions should be developed in the future.

4. Conclusion

Size-dependent temperature–pressure phase diagram of BN was established by thermodynamic theory and it can be used to explain the c-BN formation under the various experimental conditions. It was found that c-BN is more stable than h-BN in the deep nanometer scale and the triple point of c-BN, h-BN and liquid shifts toward lower temperature and pressure with decrease in the particle size. Surface stress f is the main reason that influences the formation of c-BN nuclei. The larger the value of f is, the easier the c-BN formation may be. Thereby, the value of f in the experimental condition may be first determined to open up a new preparation method of c-BN.

Acknowledgment

References

[1] M.B. Mekki, M.A. Djouadi, E. Guiot, V. Mortet, J. Pascallon, V. Stambouli, D. Bouchier, N. Mestres, G. Nouet, Surf. Coat. Tech. 116–119 (1999) 93.
[2] P.B. Mirkarimi, K.F. McCarty, D.L. Medlin, Mater. Sci. Eng. R. 21 (1997) 47.
[3] R.H. Wentorf, J. Chem. Phys. 26 (1957) 956.
[4] F.H. Bundy, R.H. Wentorf, J. Chem. Phys. 38 (1963) 1144.
[5] F.R. Corrigan, F.P. Bundy, J. Chem. Phys. 63 (1975) 3812.
[6] V.L. Solozhenko, V.Z. Turkevich, High Pressure Res. 16 (1999) 179.
[7] G. Will, G. Nover, J. Gönna, J. Solid State Chem. 154 (2000) 280.
[8] V.L. Solozhenko, V.Z. Turkevich, W.B. Holzapfel, J. Phys. Chem. B 103 (1999) 2903.
[9] V.Z. Turkevich, J. Phys. Condens. Matter 14 (2002) 10963.
[10] W. Sekkal, B. Bouhafs, H. Aourag, M. Certier, J. Phys. Condens. Matter 10 (1998) 4975.
[11] C.X. Wang, Y.H. Yang, Q.X. Liu, G.W. Yang, J. Phys. Chem. B 108 (2004) 728.
[12] V.L. Solozhenko, High Press. Res. 9 (1992) 140.
[13] H. Yamamoto, S. Matsumoto, K. Okada, J. Yu, K. Hirakuri, Diamond Relat. Mater. 15 (2006) 1357.
[14] Q. Jiang, H.M. Lu, Surf. Sci. Rep. 63 (2008) 427.
[15] Z. Zhang, J.C. Li, Q. Jiang, J. Phys. D: Appl. Phys. 33 (2000) 2653.
[16] H.W. Sheng, G. Ren, L.M. Peng, Z.Q. Hu, K. Lu, J. Mater. Res. 12 (1997) 119.
[17] F. Ercikessum, W. Andreoni, E. Tosatti, Phys. Rev. Lett. 66 (1991) 911.
[18] P. Pawlow, Z. Phys. Chem. 65 (1909) 545.
[19] K.J. Hanszen, Z. Phys 157 (1960) 523.
[20] M. Zhao, X.H. Zhou, Q. Jiang, J. Mater. Res. 16 (2001) 3304.
[21] C.X. Wang, G.W. Yang, Mater. Sci. Eng. R 49 (2005) 157.
[22] A.I. Rusanov, Surf. Sci. Rep. 58 (2005) 111.
[23] A.I. Rusanov, Surf. Sci. Rep. 23 (1996) 173.
[24] C.C. Yang, S. Li, J. Phys. Chem. C 112 (2008) 1423.
[25] Q. Jiang, Z.P. Chen, Carbon 44 (2006) 79.
[26] D.S. Zhao, M. Zhao, Q. Jiang, Diamond Relat. Mater. 11 (2002) 234.
[27] F.K. Shi, J. Mater. Res. 9 (1994) 1307.
[28] F.A. Lindemann, Phys. Z. 11 (1910) 609.
[29] A. Frenkel, E. Shasha, O. Gorodetsky, A. Voronel, Phys. Rev. B 48 (1993) 1283.
[30] Q.X. Liu, C.X. Wang, G.W. Yang, Phys. Rev. B 71 (2005) 155422.
[31] T. Yoshida, Diamond Relat. Mater. 5 (1996) 501.
[32] T. Watanabe, R. Sataka, K. Yamamoto, Thin Solid Films 516 (2008) 4462.
[33] V.L. Solozhenko, Thermochim. Acta 218 (1993) 221.

[34] S. Bohr, R. Haubner, B. Lux, Diamond Relat. Mater. 4 (1995) 714.
[35] S. Nakano, O. Fukunaga, Diamond Relat. Mater. 218 (1993) 221.
[36] C.Q. Sun, Prog. Solid State Chem. 35 (2007) 1.
[37] F.D. Fischer, T. Waitz, D. Vollath, N.K. Simha, Prog. Mater. Sci. 53 (2008) 481.
[38] G. Ouyang, C.X. Wang, G.W. Yang, Chem. Rev. 109 (2009) 4221.
[39] G. Ouyang, G.W. Yang, C.Q. Sun, W.G. Zhu, Small 4 (2008) 1359.
[40] G. Ouyang, X.L. Li, X. Tan, G.W. Yang, Phys. Rev. B 76 (2007) 193406.
[41] H.L. Duan, J. Wang, B.L. Karihaloo, Z.P. Huang, Acta Mater. 54 (2006) 2983.
[42] F.Q. Yang, J. Appl. Phys. 95 (2004) 3516.
[43] W. Liu, D. Liu, W.T. Zheng, Q. Jiang, J. Phys. Chem. C 112 (2008) 18840.
[44] B. Wang, G. Ouyang, Y.H. Yang, G.W. Yang, Appl. Phys. Lett. 90 (2007) 121905.
[45] G. Ouyang, X.L. Li, G.W. Yang, Appl. Phys. Lett. 91 (2007) 051901.